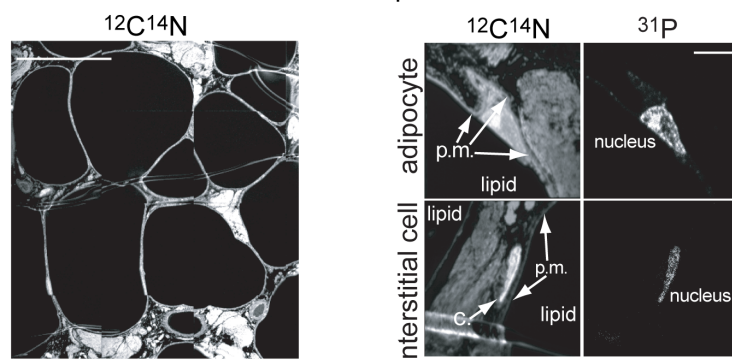


### A. Biopsy/tissue processing test unlabeled volunteer

14 gauge Temno™ biopsy system

Confirmation of tissue architecture preservation

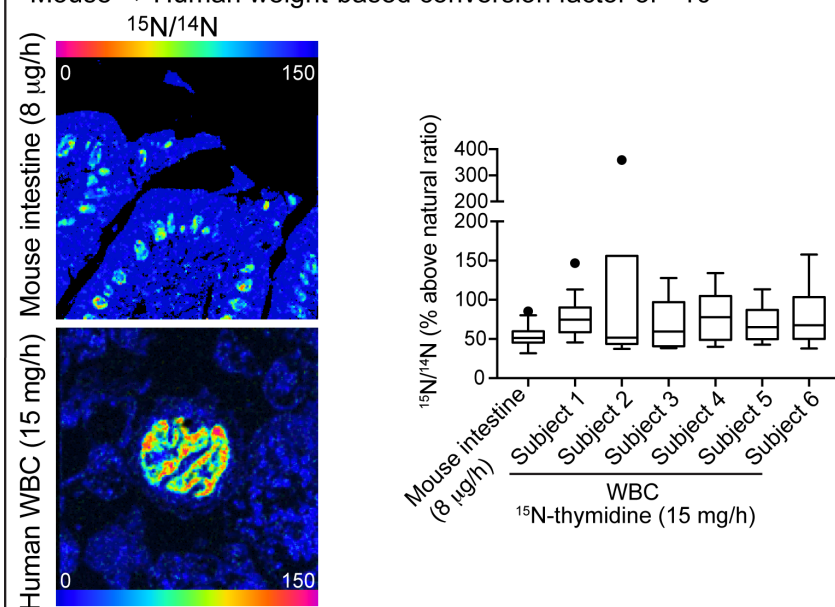


### B. Protocol 1 rationale

Effective mouse labeling rates ( $8\text{--}32\ \mu\text{g/h}$ )<sup>1,2,3</sup>

Circulating half-life ~minutes<sup>4</sup> informed choice of continuous infusion

Mouse  $\Rightarrow$  Human weight-based conversion factor of  $\sim 10^3$



### C. Protocol 2 rationale

$^{15}\text{N}$ -thymidine infusion based on protocol 1 labeling efficacy

$^2\text{H}$ -water protocol adapted from prior human D-water tracer studies<sup>5,6</sup>

3/3 subjects experienced self-limited vertigo after D-water load

Vertigo did not recur with daily maintenance doses

### D. Protocol 3 rationale

Loading protocol reduced to reduce vertigo

Maintenance dose unchanged

3/9 subjects with mild self-limited vertigo during D-water load

Vertigo did not recur with daily maintenance doses

**Supplemental Figure 1: Rationale for human stable isotope labeling protocols.**

**A)** Prior to embarking on human stable isotope labeling, we tested an approach of obtaining core biopsies from human volunteers with adequate preservation of tissue architecture. Although the softness of adipose tissue presents a challenge, we found that a 14-gauge biopsy system provided well-preserved specimens (left). Right: higher resolution mass images of an adipocyte (top) and interstitial cell (bottom). The lateral resolution enables the differentiation of adipocyte nuclei from adjacent structures based on a close association with a dominant, defining lipid droplet. The adipocyte shown on the top represents a particularly challenging and unusual example, where the lateral imaging resolution aided the discrimination of the undulating path of the adipocyte plasma membrane (p.m.) from adjacent interstitial structures. The bottom images show an example of interstitial structures, including a small capillary (c.) between the plasma membranes (p.m.) of two adjacent adipocytes. Of note, MIMS images are derived from the surface atomic layers, rather than the full thickness of the section, underscoring the concept that depth resolution exceeds the current maximal lateral resolution of approximately 30 nm. Therefore, although the sample sputtering process is destructive of the surface atomic layers, the 0.5  $\mu\text{m}$  sections utilized in this study provide abundant depth for follow-up higher resolution analyses.

**B)** We designed the  $^{15}\text{N}$ -thymidine labeling protocols, informed by this published experience and in combination with our experience conducting labeling studies in mice(1-3). The pharmacokinetics of thymidine in circulation were defined by studies exploring the utility of supra-physiological thymidine to inhibit the cell cycle in cancer patients, at doses that were at least 3 orders of magnitude higher than those used in these studies(4). Because the half-life in circulation is on the order of minutes, we opted to administer a bolus followed by a continuous infusion, reasoning that such an approach should lead to a stable label exposure over the desired labeling period. The  $^{15}\text{N}$ -thymidine dose was based on an approximate mouse to human weight-based conversion. In our prior murine studies, the small intestine provided an efficient

tissue in which to validate labeling protocols, due to its rapid turnover(1-3). We reasoned that peripheral leukocytes provided the closest and most easily accessible corollary tissue for such validation in humans. The top left image shows an example of a small intestinal villus obtained after continuous administration of  $^{15}\text{N}$ -thymidine to a mouse by osmotic minipump. A human leukocyte demonstrates a qualitatively similar, and robust, degree of labeling after continuous intravenous infusion of the selected dose of  $^{15}\text{N}$ -thymidine. The Tukey box plots on the right suggest achievement of similar levels of labeling in human leukocytes as compared to murine epithelial cells.

**C)** Unlike the  $^{15}\text{N}$ -thymidine method, precedent existed in the literature to inform our  $^2\text{H}$ -water dosing protocol(5, 6). We first opted for a rapid oral  $^2\text{H}$ -water load (400 ml) to achieve rapid onset of labeling analogous to the intravenous bolus of  $^{15}\text{N}$ -thymidine. All 3 subjects experienced self-limited vertigo lasting several hours, a side effect attributable to the sensitivity of the inner ear to changes in the fluid mass. Importantly, the vertigo did not recur with administration of daily maintenance doses (60 ml).

**D)** The experience of vertigo with  $^2\text{H}$ -water loading prompted us to reduce the load for the long-term labeling study (Protocol 3: 4 wks  $^2\text{H}$ -water labeling). Subjects were administered a total of 240 ml in divided 80 ml doses over 6 hours. With this approach only 3/9 subjects experienced vertigo and the severity was generally less than that reported by the subjects after a 400 ml oral bolus.

### **Supplemental References:**

1. Steinhauser, M.L., Bailey, A.P., Senyo, S.E., Guillermier, C., Perlstein, T.S., Gould, A.P., Lee, R.T., and Lechene, C.P. 2012. Multi-isotope imaging mass spectrometry quantifies stem cell division and metabolism. *Nature* 481:516-519.
2. Kim, S.M., Lun, M., Wang, M., Senyo, S.E., Guillermier, C., Patwari, P., and Steinhauser, M.L. 2014. Loss of white adipose hyperplastic potential is associated with enhanced susceptibility to insulin resistance. *Cell Metab* 20:1049-1058.

3. Senyo, S.E., Steinhauser, M.L., Pizzimenti, C.L., Yang, V.K., Cai, L., Wang, M., Wu, T.D., Guerquin-Kern, J.L., Lechene, C.P., and Lee, R.T. 2013. Mammalian heart renewal by pre-existing cardiomyocytes. *Nature* 493:433-436.
4. O'Dwyer, P.J., King, S.A., Hoth, D.F., and Leyland-Jones, B. 1987. Role of thymidine in biochemical modulation: a review. *Cancer Res* 47:3911-3919.
5. Neese, R.A., Misell, L.M., Turner, S., Chu, A., Kim, J., Cesar, D., Hoh, R., Antelo, F., Strawford, A., McCune, J.M., et al. 2002. Measurement in vivo of proliferation rates of slow turnover cells by  $2\text{H}_2\text{O}$  labeling of the deoxyribose moiety of DNA. *Proc Natl Acad Sci U S A* 99:15345-15350.
6. Strawford, A., Antelo, F., Christiansen, M., and Hellerstein, M.K. 2004. Adipose tissue triglyceride turnover, de novo lipogenesis, and cell proliferation in humans measured with  $2\text{H}_2\text{O}$ . *Am J Physiol Endocrinol Metab* 286:E577-588.